B-DNA to Z-DNA Structural Transitions in the SV40 Enhancer: Stabilization of Z-DNA in Negatively Supercoiled DNA Minicircles†

Elliott A. Gruskin‡,§ and Alexander Rich*,§

Department of Biology, Massachusetts Institute of Technology, Cambridge, Massachusetts 02139, and Department of Biochemistry, United States Surgical Corporation, 150 Glover Avenue, Norwalk, Connecticut 06856

Received August 12, 1992; Revised Manuscript Received December 10, 1992

ABSTRACT: During replication and transcription, the SV40 control region is subjected to significant levels of DNA unwinding. There are three, alternating purine-pyrimidine tracts within this region that can adopt the Z-DNA conformation in response to negative superhelix density: a single copy of ACACACAT and two copies of ATGCATGC. Since the control region is essential for both efficient transcription and replication, B-DNA to Z-DNA transitions in these vital sequence tracts may have significant biological consequences. We have synthesized DNA minicircles to detect B-DNA to Z-DNA transitions in the SV40 enhancer, and to determine the negative superhelix density required to stabilize the Z-DNA. A variety of DNA sequences, including the entire SV40 enhancer and the two segments of the enhancer with alternating purine-pyrimidine tracts, were incorported into topologically relaxed minicircles. Negative supercoils were generated, and the resulting topoisomers were resolved by electrophoresis. Using an anti-Z-DNA Fab and an electrophoretic mobility shift assay, Z-DNA was detected in the enhancer-containing minicircles at a superhelix density of –0.05. Fab saturation binding experiments demonstrated that three, independent Z-DNA tracts were stabilized in the supercoiled minicircles. Two other minicircles, each with one of the two alternating purine-pyrimidine tracts, also contained single Z-DNA sites. These results confirm the identities of the Z-DNA-forming sequences within the control region. Moreover, the B-DNA to Z-DNA transitions were detected at superhelix densities observed during normal replication and transcription processes in the SV40 life cycle.

Important regulatory mechanisms may be triggered by changes in DNA topology. DNA unwinding occurs at the initiation of SV40 replication with the binding of the large T antigen (Stahl et al., 1986; Dean et al., 1987b; Dodson et al., 1987; Bullock et al., 1989; Roberts, 1989; Gutierrez et al., 1990; Dean & Hurwitz, 1991). DNA supercoiling is also a factor at the completion of replication in that the initial products of replication are topologically unwound (Bullock et al., 1989). Complex changes in DNA topology accompany transcription. Positive supercoils are formed in front of RNA polymerase, and negative supercoils behind it (Wu et al., 1988). When two transcription units are oriented in opposite orientations, as is the case for the SV40 enhancer, the DNA between them is subjected to high levels of negative superhelix density.

One of the most dramatic effects of DNA unwinding is the transition of B-DNA to Z-DNA. B-DNA to Z-DNA transitions that occur as a result of the significant changes in superhelix density during replication and transcription may play an important regulatory role. We have set out to investigate Z-DNA-forming sequences within the SV40 enhancer through the use of DNA minicircles. A strategy was developed to determine the number of independent Z-DNA sequence tracts, and the negative superhelix density required to stabilize the Z-DNA conformation.

A variety of immunological and sequence analyses have demonstrated that the SV40 genome contains several sites capable of adopting the left-handed, Z-DNA conformation. Immunological studies mapped three Z-DNA sites in the viral control sequences (Nordheim & Rich, 1983; Zarling et al., 1984; Hagen et al., 1985; Nordheim et al., 1987). Since there are three sequence tracts with eight base pair, alternating purine-pyrimidine sequences within the control region, it was assumed that these must be the Z-DNA-forming sites. Here DNA minicircles have been employed to analyze the specific sequences within the SV40 enhancer that adopt the Z-DNA conformation. In addition, the negative superhelix density required to convert the sequences to the Z-DNA configuration was determined.

DNA minicircles have emerged as powerful tools to study DNA structure, topology, and DNA interactive proteins. DNA fragments with self-complementary cohesive termini are used to generate circles as small as several hundred base pairs. Because of their small size, DNA minicircles have been used as substrates for gel electrophoresis mobility shift assays to study protein–DNA interactions. For example, the interactions of *Eco*RI, CAP, and the *lac* repressor with cognate binding sites have been investigated with minicircles that have different superhelix densities (Douc-Rasy et al., 1989). In addition, the activity of DNA gyrase (Bates & Maxwell, 1989), the DNA unwinding capacity of SV40 large T antigen (Dean & Hurwitz, 1991), and the interaction of Z-DNA antibodies with minicircles containing sequences that can adopt the

† This research was supported by grants from the National Institutes of Health, the American Cancer Society, the National Science Foundation, the Office of Naval Research, and the National Aeronautics and Space Administration. E.G. was supported by a postdoctoral fellowship from the National Institutes of Health.

* Author to whom correspondence should be addressed.
‡ United States Surgical Corp.
§ Massachusetts Institute of Technology.

0006-2960/93/0432-2167$04.00/0 © 1993 American Chemical Society

Table I: Summary of DNA Minicircles

mini-circle	parent plasmid	size (bp)	description
Z^-	pUC-EG4	270	negative control for Z-DNA
Z^+	pEGAR	285	positive control for Z-DNA: contains 26 bp alternating CG sequence tract
SV	pUC-EG5	372	contains SV40 sequences including origin of replication and enhancer element
SVZ_1	pUC-EG7	291	contains SV40 sequence 5′TAATTGAG-**ATGCATGC**-TTTGCATA3′ [a]
SVZ_2	pDG-2	291	contains SV40 sequence 5′CCTAACTG-**ACACACAT**-TCCACAG3′ [b]

[a] Sequence tract begins at position 119 in the SV40 genome. Bold-face type indicates the alternating purine-pyrimidine sequence tracts. [b] Sequence tract begins at position 250 in the SV40 genome. Bold-face type indicates the alternating purine-pyrimidine sequence tracts.

Z-DNA conformation (Nordheim & Meese, 1988) have been analyzed with DNA minicircles.

It is difficult to study a single Z-DNA tract within a large plasmid that contains multiple Z-DNA-forming sequences. However, with DNA minicircles, the influence of other sequence tracts can be excluded to understand the behavior of a specific subset of the genome. Since minicircles contain several hundred base pairs, rather than several thousand, as in a conventional plasmid, the contributions of specific sequences to the overall structure and topology are more readily observed. This advantage is especially useful for the study of Z-DNA: With DNA minicircles, the conversion from B-DNA to Z-DNA can be stabilized by negative supercoils (Singelton et al., 1982; Peck et al., 1982, 1986) instead of chemical means such as bromination (Moller et al., 1984). Supercoils have been shown to stabilize B-DNA to Z-DNA transitions of 12 base pair, alternating purine-pyrimidine sequence tracts in conventional plasmids (Rahmouni & Wells, 1989). However, a plasmid several kilobases in size has sufficient sequence complexity such that many Z-DNA potential sequences coexist. Since the energy requirements for many of the B-DNA to Z-DNA transitions are nearly equivalent, any individual transition is difficult to detect. Long-range interactions between competing domains have been observed for plasmids that contain several, independent, purine-pyrimidine sequence tracts (Ellison et al., 1987). The SV40 genome is similar in that many small stretches of Z-DNA, as well as other structures such as triple helices and hairpin loops, can compete for the energy stored as negative supercoils. Individual sequence tracts exist in a B-DNA and Z-DNA equilibrium that is affected by all the other sequences that vie for stabilization energy.

Several minicircles were constructed for the work reported here (see Table I). All of the minicircles were synthesized as relaxed circles and then supercoiled by treatment with topoisomerase I in the presence of ethidium bromide. The resulting topoisomers, which differed by single, supercoil increments, were resolved by electrophoresis in the presence of chloroquine. Identical samples of the minicircles were incubated with the Fab[1] part of a Z-DNA-specific monoclonal antibody (Moller et al., 1982) and subjected to an electrophoretic mobility shift assay. A comparison of the chloroquine gels to the mobility shift experiment was used to ascertain which topoisomers contained Z-DNA. Saturation binding experiments of Fab with the maximally supercoiled minicircles were used to determine the number of independent, Z-DNA-forming sites within each minicircle. Through this strategy, Z-DNA-forming sequences were detected, and the negative superhelix density required to stabilize the Z-DNA was determined.

[1] Abbreviations: BSA, bovine serum albumin; DTT, dithiothreitol; EDTA, ethylenediaminetetraacetic acid; Fab, Fab fragment of a monoclonal antibody.

MATERIALS AND METHODS

Plasmids. DNA fragments with self-complementary cohesive termini were used to synthesize the DNA minicircles (Table I). The plasmid pUC-EG4 was constructed as follows. The *Sph*I site of pUC-18 was deleted by digestion with *Pst*I and *Hin*dIII followed by recircularization (deletion of this *Sph*I site was important since this sequence is found within the SV40 enhancer). An oligonucleotide containing *Pst*I, *Hin*dIII, and *Aat*II sites was ligated into the unique *Eco*RI site. The plasmid pUC-EG5 was constructed by ligation of the 798 bp, *Taq*I–*Kpn*I fragment of SV40 into the *Nar*I and *Kpn*I sites of pUC-EG4. The plasmid pEGAR was constructed by ligation of a 45 bp *Kpn*I–*Bam*HI fragment of pME-A, that contains a $(CG)_{13}$ sequence, into the corresponding sites of pUC-EG4. To construct plasmids pUC-EG7 and pDG-2, oligonucleotides were synthesized that contain the SV40 sequences flanked by *Kpn*I and *Bam*HI sites. The oligonucleotides were ligated into the corresponding sites of pUC-EG4.

Synthesis and Purification of DNA Minicircles. The minicircle synthesis, and subsequent analyses, employed modifications of previously published methods (Nordheim & Meese, 1988). The DNA fragments were end-labeled with [γ-^{32}P]ATP. The ligation reactions were performed at a DNA concentration of 1 μg/mL: The ^{32}P-labeled DNA in 50 μL of H_2O was heated to 65 °C to disrupt intermolecular hybridizations and then added to a 1.95-mL ligation reaction mixture at 4 °C. The resulting 2-mL reactions consisted of 2 μg of ^{32}P-labeled DNA fragment, 1 mM ultrapure ATP (Pharmacia), 100 μg/mL BSA, 20 mM DTT, 50 mM Tris-HCl (pH 7.8), 10 mM $MgCl_2$, and 10 000 units of T4 DNA ligase (New England Biolabs, 2 000 000 units/mL). The ligation reaction was maintained at 4 °C for 16 h. At the conclusion of the ligation reaction, 10 μL of 0.5 M EDTA, 40 μL of 2.5 M KCl, and 2.5 μL of topoisomerase I (New England Biolabs) were added, and the reaction was continued at 37 °C for 60 min. The DNA was purified from the ligation reaction mixture by anion-exchange chromatography with Qiagen columns (Qiagen Corp.).

The ligation reaction generated a variety of DNA species. Solubilizable polyacrylamide gels were employed to purify the unit-length circular subpopulation. The DNA was subjected to electrophoresis through a 1.5-mm, 4%, 30:1 acrylamide/bis(acrylylcystamine) (BAC)–polyacrylamide gel in 90 mM Tris–borate/2 mM EDTA (RB). Electrophoresis was performed with a Bio-Rad Protean gel system modified for buffer recircularization. Chloroquine at 10 mg/mL was added to a final concentration of 20 μg/mL in both the gel and the electrophoresis running buffer. Electrophoresis was carried out at 100 V for 12 h at 4 °C. At the completion of the gel run, the glass plates were carefully separated, and the gel was left on one of the plates, covered with plastic film, and then exposed to X-ray film at 25 °C for 2–5 min with an intensifying screen. The resulting autoradiograph was used as a template to identify the positions of the DNA within the gel. DNA was purified from the solubilizable gel matrix by modifications of published procedures (Hansen et al., 1979; Hansen, 1981; Marotta et al., 1982).

The specific DNA bands that corresponded to the unit-length circle for each minicircle had to be identified from

among the ligation products. The DNA in each band in the solubilizable gels was purified. Each DNA sample was treated with topisomerase I in the presence of 0.5 μg/mL ethidium bromide (as described in the next section). The samples were resolved by electrophoresis through 1.5-mm, 4%, 30:1 acrylamide/PDA gels in RB at 100 V for 12 h at 4 °C. A shift in the electrophoretic mobility was diagnostic for a circular species. The mobility of the circular forms generated by ligations of the Z^+- and SV-minicircles was coincident with the mobility of the linear dimers. To further purify the minicircles, a second round of electrophoresis was required; however, chloroquine was excluded. Under these conditions the mobility of the minicircle was shifted relative to the linear dimer. It was then possible to purify just the minicircle form. The efficiency of circularization varied from approximately 30% for SV-minicircles to 10–20% for the other minicircles.

Supercoiling Reactions and Resolution of Topoisomers. Negative superhelix denisty was introduced into the circular DNA by treatment with topoisomerase I in the presence of ethidium bromide. Purified minicircles, with zero supercoils, were incubated for 60 min in a 50-μL reaction consisting of 50 mM Tris-HCl (pH 7.5), 50 mM KCl, 10 mM $MgCl_2$, 0.1 mM EDTA, 0.5 mM DTT, 30 μg/mL BSA, and ethidium bromide at the indicated concentrations (0–2 μg/mL). The DNA was phenol-extracted, precipitated with 10 μg of poly(dI-dC), and resuspended in 10 mM Tris-HCl (pH 8.0)/1 mM EDTA. The resulting topoisomers were resolved by electrophoresis through 1.5-mm, 4%, 30:1 acrylamide/PDA gels in RB. Chloroquine at 20 μg/mL was present in both the gel and electrophoresis running buffer. Electrophoresis was carried out at 100 V for 12 h at 4 °C. The gels were dried under vacuum and exposed to X-ray film for 12 h at −80 °C using two intensifying screens.

Gel Electrophoresis Mobility Shift Assays. The presence of Z-DNA in minicircles was determined by the binding of the Fab fragment of the Z-DNA-specific monoclonal antibody Z-22 (Moller et al., 1982; Nordheim et al., 1986): To limit nonspecific DNA binding, all of the reaction components, with the exception of the DNA minicircles, were incubated for 15 min at 4 °C. Upon the addition of minicircle DNA, the reaction, which consisted of the indicated concentration of Fab, 100 pg of minicircle DNA (approximately 5000 cpm), 1.5 μg of poly(dI-dC), 2 mM Tris-HCl (pH 8.0), 10 mM EDTA, 50 mM NaCl, 10% glycerol, 100 μg/mL BSA, and 10 mM DTT, was shifted to 25 °C for 60 min. A second set of reactions was carried out without the addition of Fab to serve as a control. The reactions were loaded directly onto 1.5-mm, 4%, 30:1 polyacrylamide/PDA gels in RB and subjected to electrophoresis at 200 V for 6 h at 4 °C. The gels were dried under vacuum and exposed to X-ray film for 12 h at −80 °C using two intensifying screens.

RESULTS

Z^--Minicircle. As was the case for all the minicircles tested, the gel system for the electrophoretic mobility shift analysis was unable to resolve individual topoisomers (Figure 1, panel A). However, the system clearly resolved free minicircles from Fab-bound minicircles (Figure 1, panel B). A comparison of Figure 1, panel B, to Figure 1, panel C, demonstrates that the first Fab-induced mobility shift is coincident with the emergence of the topoisomer in lane 11. Since the topoisomers were generated by treatment with topoisomerase I and ethidium bromide, the superhelix density of each successive band differed by one supercoil. A chloroquine concentration

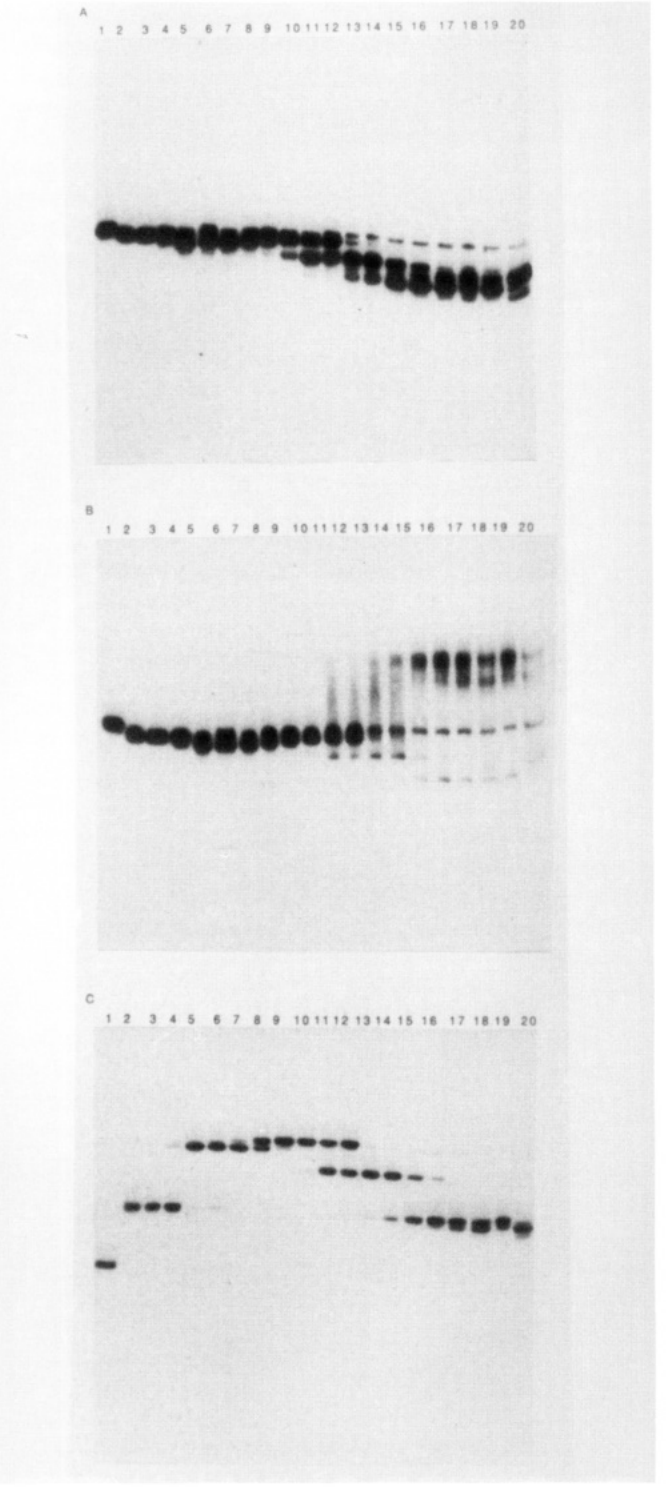

FIGURE 1: Analysis of the Z^--minicircle. Topologically relaxed minicircles were synthesized and supercoiled by treatment with topoisomerase I in the presence of ethidium bromide (see Materials and Methods). In all three panels, lanes 1–20 represent the different concentrations of ethidium bromide used in the supercoiling reactions: 0.00, 0.05, 0.10, 0.15, 0.20, 0.25, 0.30, 0.35, 0.40, 0.45, 0.50, 0.60, 0.70, 0.80, 1.00, 1.20, 1.40, 1.60, 1.80, and 2.00 μg/mL, respectively. Electrophoresis and autoradiography were performed as described under Materials and Methods. Panels A and B comprise the Fab binding experiment. Panel A shows the electrophoretic mobility of the Z^--minicircles in the absence of Fab. Panel B shows the same Z^--minicircle topoisomers after the addition of 5 μg of Fab per lane. Changes in the bands are a result of the retardation of the electrophoretic mobility of specific Z^--minicircle topoisomers that have bound to Fab. Panel C shows the topoisomer resolution experiment in which the Z^--minicircle topoisomers were resolved in the presence of chloroquine.

was determined empirically that resulted in the maximal mobility of the relaxed minicircle (Figure 1, panel C, lane 1), and allowed sufficient resolution of the more highly supercoiled species. The result was the expected bell-shaped distribution of topoisomers: The chloroquine intercalated into the DNA such that a specific number of positive supercoiles were generated. The band in lane 1, Figure 1, panel C, was the relaxed topoisomer of the minicircle; however, in the presence of chloroquine, it was the most positively supercoiled species. The mobility of the minicircles in successive lanes first decreased, which is the result of increased negative superhelix density, but decreased positive superhelix density in the presence of chloroquine. The minicircle with the slowest mobility was at the top of the bell-shaped distribution. This species contained –2 supercoils; however, in the gel the DNA was actually at a zero superhelix density. The mobility of the minicircles after this point increased, which indicated that the minicircles were negatively supercoiled in the presence of chloroquine. Thus, the number of supercoils can be determined by assigning 0 supercoils for the minicircles in lane 1, and then each successive band would have 1 additional negative supercoil. Therefore, the Z^--minicircle was supercoiled to a maximum of 6 negative supercoils which corresponds to a superhelix density of –0.22. The emergence of the band shift caused by the Fab fragment was coincident with the appearance of the –4 topoisomer. This topoisomer has a superhelix density of –0.15.

The Fab binding did not result in discrete shifted bands; rather, a degenerate pattern of bands emerged. This distribution of bands could have resulted from multiple Z-DNA sites on each minicircle which competed for Fab binding. This effect has been observed in other Z-DNA detection methods in instances where sequences were analyzed that were not particularly favorable for B-DNA to Z-DNA structural transitions. Many independent sequences have high, but isoenergetic requirements for conversion to Z-DNA. The Fab fragment can bind to any of these sites within the population of minicircles, thus generating a variety of shifted species. This interpretation will become apparent upon the perusal of the same experiment performed on Z^+-minicircles.

Z^+-Minicircle. The Z^- and the Z^+-minicircles are identical with the exception of a $(CG)_{13}$ insert. However, the effects of this insert on the results were dramatic (Figure 2). Although the resolution capacity of the gel in Figure 2, panel A, was limited, it was clear that a more rapidly migrating topoisomer was generated in the sample in lane 4 that binds the Fab fragment (Figure 2, panel B, lane 5). This result was diagnostic for the conversion of the $(CG)_{13}$ insert to the Z-DNA conformation. The resolution of the topoisomers in Figure 2, panel C, demonstrates that the B-DNA to Z-DNA conversion occurs with the addition of one superhelical turn to the minicircle, which corresponds to a superhelix density of –0.04. The distribution of topoisomers for the Z^+-minicircle differed significantly from that oberved for the Z^--minicircle. The most notable difference was the discontinuity in the bell-shaped distribution of topoisomers in lanes 13–20. The discontinuity can be explained by a B-DNA to Z-DNA transition within the $(CG)_{13}$ sequence which absorbed one negative supercoil. Thus, there was a transition from a species with a more rapid migration to a species with a slower migration observed in lanes 18–20. However, the three topoisomers observed in lane 16 suggest that other supercoil-induced structural transitions such as hairpin loops, bulging, or kinking may have occurred. Although there may be several competing structures, the predominant conformation of the $(CG)_{13}$ sequence at high supercoils is probably Z-DNA.

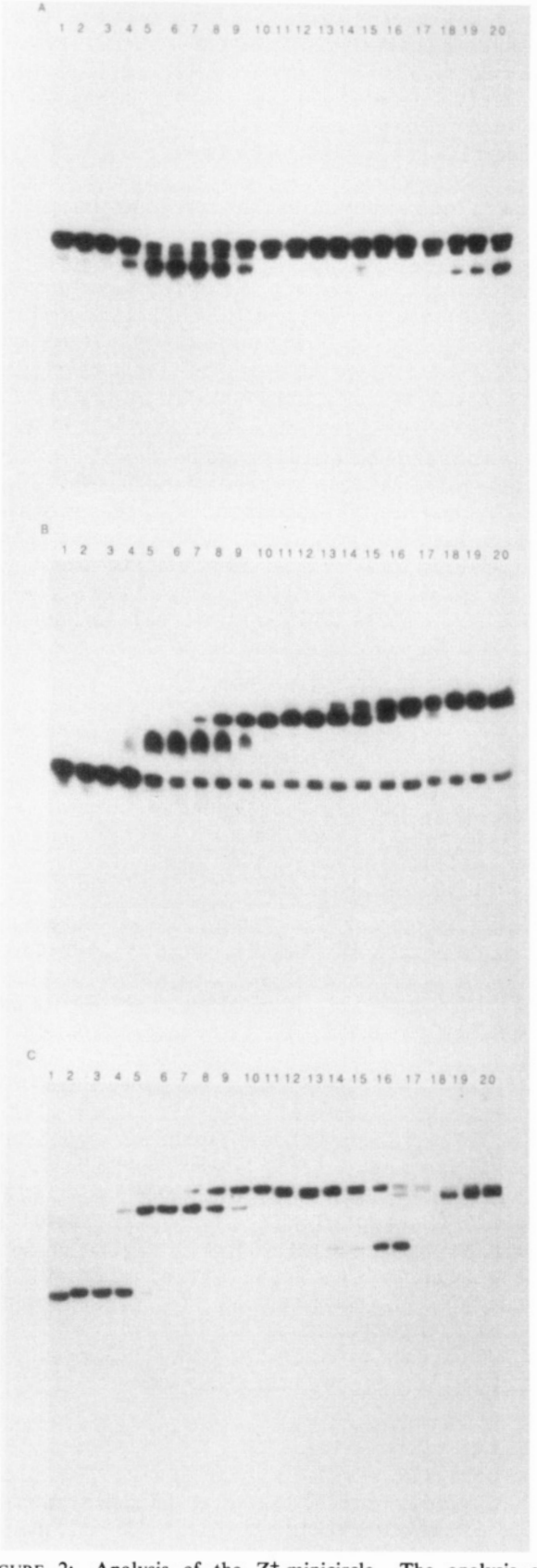

FIGURE 2: Analysis of the Z^+-minicircle. The analysis and identification of the lanes are identical to those shown in Figure 1. Panel A, Z^+-minicircle topoisomers in the absence of Fab; panel B, Z^+-minicircle topoisomers after the addition of 5 μg of Fab per reaction; panel C, resolution of the Z^+-minicircle topoisomers in the presence of chloroquine.

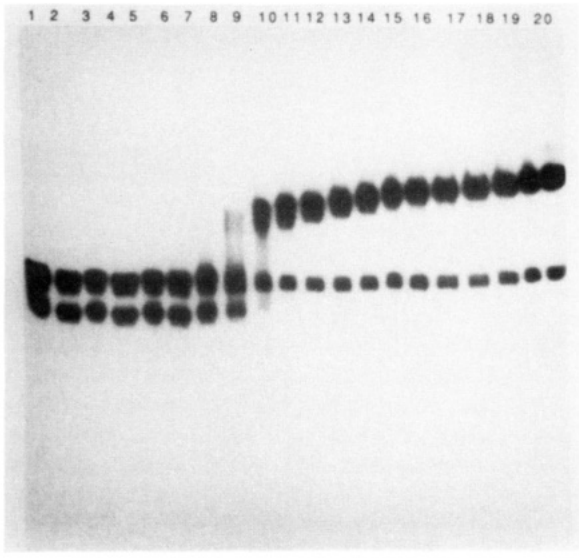

FIGURE 3: Saturation binding experiment of Z^+-minicircles and Fab. The maximally supercoiled Z^+-minicircle shown in Figure 2, panel A, lane 20, was subjected to a saturation binding experiment (see Materials and Methods). In lanes 1–20, 100 pg of Z^+-minicircle was incubated with the following amounts of Fab: 0.00, 38 ng, 76 ng, 150 ng, 305 ng, 610 ng, 1.2 pg, 2.4 pg, 4.8 pg, 9.8 pg, 20 pg, 39 pg, 78 pg, 160 pg, 310 pg, 630 pg, 1.3 μg, 2.5 μg, 5.0 μg, and 10 μg, respectively.

The apparent transition to the Z-DNA conformation occurred with the addition of one negative supercoil to the –1 topoisomer, for a total of two negative supercoils, and a negative superhelix density of –0.07. However, the band shift experiment demonstrated that the –1 topoisomer contained Z-DNA. An explanation for this apparent discrepancy is that the Fab fragment influenced the equilibrium position between the B-DNA and Z-DNA conformations of the –1 topoisomer. The addition of one negative supercoil could have been sufficient to shift the equilibrium toward the Z-DNA configuration. The Fab could have trapped the Z-DNA by binding to it. Band shifts were not generated with the relaxed topoisomer because the B-DNA to Z-DNA equilibrium in these topoisomers would have strongly favored the B-DNA conformation. This conclustion is consistent with previous experiments in which anti-Z-DNA antibodies stabilized Z-DNA in relaxed linear plasmids with poly(GC) inserts (Lafer et al., 1985a).

The gel shift and topoisomer resolution data demonstrated that the Z-DNA transition occurred between the –1 and –2 topoisomer. A band shift was also observed for each successive topoisomer with increased negative superhelix density. The mobility of the shifted band changed in concert with the appearance of each new topoisomer. The heterogeneity could have resulted from multiple Fab fragments bound to the Z-DNA within a minicircle, or from differences in the mobilities of the minicircles prior to Fab binding. To resolve these possibilities, a saturation binding experiment was performed in which minicircles at the highest superhelix density (Figure 2, lane 20) were incubated with increased concentrations of Fab. The results (Figure 3) demonstrated that at saturation binding, only one Fab could occupy the Z-DNA site on each minicircle. This result is in contrast to those reported previously (Runkel & Nordheim, 1986) in which bivalent binding of the intact antibody to a poly(CG) sequence was observed. However, in that study, intact antibody was used. It is likely that independent Fab molecules bound the Z-DNA in such a way that precluded another Fab from binding to a nearby site on the same stretch of Z-DNA. Therefore, since only one Fab can bind to each minicircle, the different band shift mobilities, observed in Figure 2, panel B, must have originated from the different mobilities of the unbound minicircles.

Unlike the results observed for the Z^--minicircle, discrete band shifts were observed for the Z^+-minicircle. Furthermore, the observation that only one Fab can bind to the $(CG)_{13}$ site offers additional proof that the degenerate distribution of Fab-induced band shifts observed for Z^--minicircles at high superhelix density was the result of independent Z-DNA sites within the same minicircle. The transition of the $(CG)_{13}$ sequence in the Z^+-minicircle to the Z-DNA configuration required relatively low negative superhelix density. Thus, although the Z^+-minicircle was nearly identical to the Z^--minicircle, the $(CG)_{13}$ sequence acted as an energy sink that prevented the emergence of the degenerate Z-DNA sites that were observed in the Z^--minicircle. These results underscore the dramatic effects that a short Z-DNA-forming sequence has on the properties of a larger set of sequences. The $(CG)_{13}$ sequence absorbs negative supercoils upon its conversion to Z-DNA, which in turn limits the negative superhelix density subjected on other sequences.

SV-Minicircle. The minicircle system provided a unique opportunity to study Z-DNA within the SV40 enhancer. Through an analysis of the enhancer sequence in isolation in a minicircle, it was possible to get a more definitive understanding of the conversion of the three eight base pair alternating purine-pyrimidine sequences to the Z-DNA configuration. The larger size of the SV-minicircle, relative to the ones described previously, resulted in a different electrophoretic mobility pattern. As shown in Figure 4, panel A, the mobility of the minicircles was increased with added superhelix density. However a pair of bands with a slower electrophoretic mobility was observed in each lane. These doublets were observed in every preparation of SV-minicircles. The resolution of the topoisomers in Figure 4, panel C, provided information on the identity of these doublets. Although a pair of doublets was observed in the absence of chloroquine, in the presence of chloroquine only a single band was observed as the species with the slowest electrophoretic mobility. A trace level of this band was observed in each lane on the topoisomer resolution gels. Furthermore, the magnitude of this band increased as the time between the preparation of the topoisomers and the topoisomer analysis was extended (data not shown). Therefore, this band represented minicircles with one or more single-strand gaps. Since the minicircles in this subpopulation had single-strand gaps, the electrophoretic mobility would have been unaffected by the presence of chloroquine. A doublet at this position in the absence of chloroquine demonstrates that one of the two bands was the relaxed form and the other was the nicked form.

The band shift analysis detected Z-DNA in the –2 topoiosmer which has a superhelix density of –0.05 (Figure 4, panel B). Although the results from the analysis of the Z^+-minicircle demonstrated that one Fab fragment could bind to each eight base pair Z-DNA sequence, the gel in Figure 4, panel B, could not detect multimeric Fab binding. The electrophoretic mobility of the free minicircles was sufficiently complex to obscure the interpretation. To determine the number of Fab fragments bound to the minicircles and in turn the number of independent Z-DNA sites, the most highly supercoiled minicircle preparation (Figure 4, lane 20) was incubated with different concentrations of the Fab fragment (Figure 5). In contrast to the saturation Fab binding experiment for the Z^+-minicircle, evidence of multimeric Fab

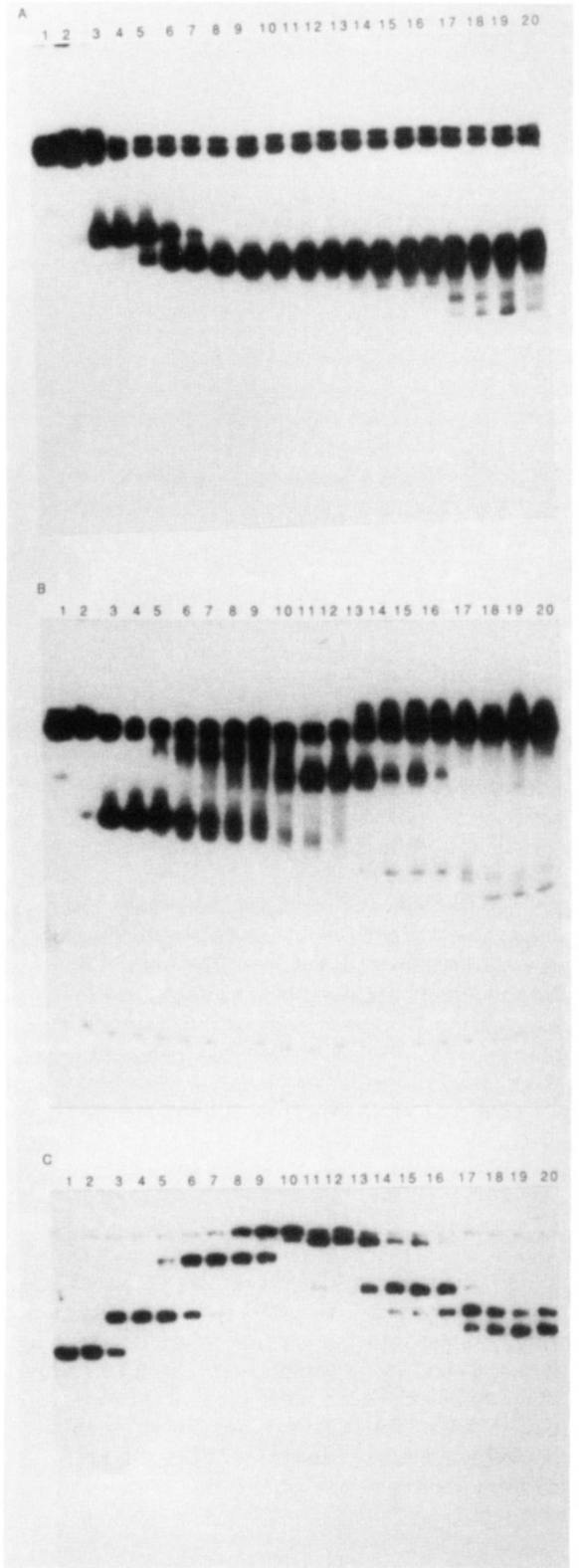

FIGURE 4: Analysis of the SV-minicircle. The analysis is identical in format to that described in Figure 1. Panel A shows the SV-minicircle topoisomers in the absence of Fab. Panel B shows the SV-minicircle topoisomers after the addition of 5 μg of Fab per reaction. Panel C shows the resolution of SV-minicircle topoisomers in the presence of chloroquine.

binding was observed. Monomeric, dimeric, and trimeric complexes were resolved. A plot of the electrophoretic mobility of the complexes versus the assumed molecular weight resulted in a straight line (data not shown). Although the Fab and minicircle concentrations in this experiment were identical to those used in the same experiment on the Z^+-minicircle, Fab

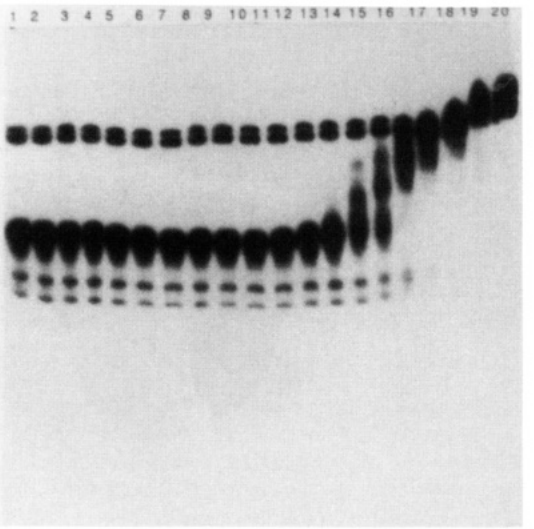

FIGURE 5: Saturation binding experiment of SV-minicircle and Fab. The maximally supercoiled SV-minicircle shown in Figure 4, panel A, lane 20, was subjected to a saturation binding experiment. The amount of Fab added in each lane is identical to that described in Figure 3.

binding was not detected until much higher concentrations of Fab. The lower affinity could be the result of an inherent sequence preference of the Fab for poly(GC) sequences, or a steric hindrance associated with the binding of the Fab fragment to the much shorter stretches of Z-DNA found in the SV-minicircle.

SVZ_1- and SVZ_2-Minicircles. The analysis of the SV-minicircle confirmed the previously published results for the conversion to Z-DNA of three independent sequences within the SV40 enhancer. To confirm the specific identity of the three Z-DNA sites as the two copies of ATGCATGC and single copy of ACACACAT, minicircles were prepared that contained each of the eight base pair alternating purine-pyrimidine sequences (including eight base pairs of SV40 sequence on each side of the eight base pair stretch). The results from the analysis of the SVZ_1-minicircle (Figure 6) and the SVZ_2-minicircle (Figure 7) were similar. Both bound Fab, which resulted in unique bands with retarded electrophoretic mobility. This result is consistent with monovalent binding of the Fab fragment to a specific sequence on each minicircle. However, the superhelix density that induced Fab binding was different for the two minicircles. The band shift observed in SVZ_2-minicircles originated from the –3 topoisomer with a negative superhelix density of –0.11. In contrast, a band shift was not observed for SVZ_1-minicircles until the –4 topoisomer with a negative superhelix density of –0.14. Therefore, the energy required to stabilize the Z-DNA conformation of the ACACACAT sequence was less than that required for the ATGCATGC sequence. However, both sequences adopted the Z-DNA conformation at greater negative superhelix densities than were observed for Z-DNA formation in the SV-minicircle.

DISCUSSION

Virtually all biochemical processes involving DNA have significant effects on DNA topology. Among all the topological variations and alternate helix geometries, none are as divergent from the standard B-DNA conformation as Z-DNA. In a transition from B-DNA to Z-DNA, the relative orientation of individual bases is changed, and the overall topology of the DNA is altered. A variety of promoters and enhancers have

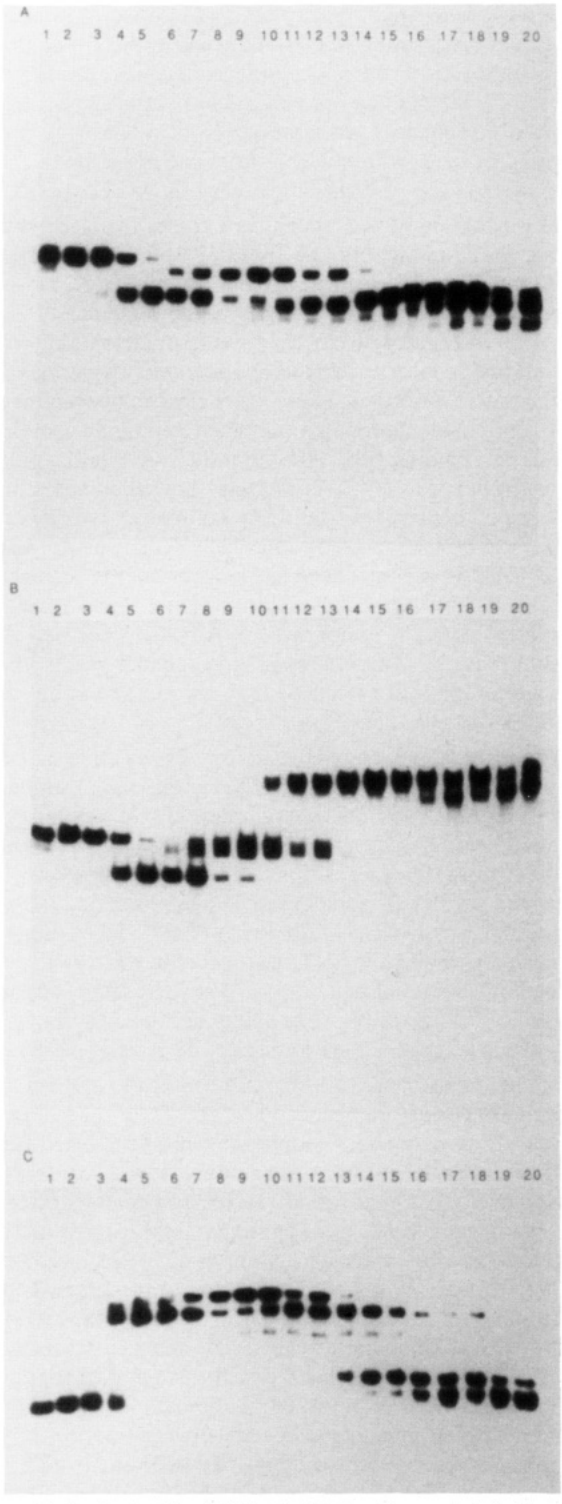

FIGURE 6: Analysis of the SVZ_1-minicircle. The analysis is identical in format to that described in Figure 1. Panel A shows the SVZ_1-minicircle topoisomers in the absence of Fab. Panel B shows the SVZ_1-minicircle topoisomers after the addition of 5 μg of Fab per reaction. Panel C shows the resolution of SVZ_1-minicircle topoisomers in the presence of chloroquine.

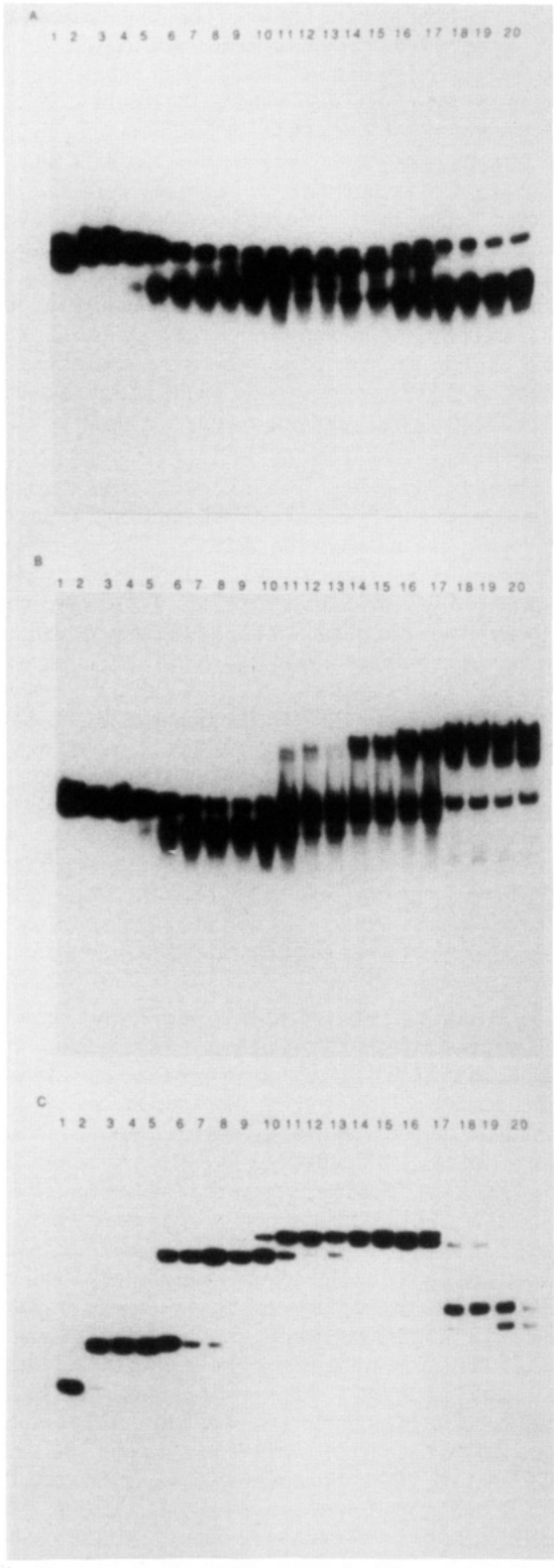

FIGURE 7: Analysis of the SVZ_2-minicircle. The analysis is identical in format to that described in Figure 1. Panel A shows the SVZ_2-minicircle topoisomers in the absence of Fab. Panel B shows the SVZ_2-minicircle topoisomers after the addition of 5 μg of Fab per reaction. Panel C shows the resolution of SVZ_2-minicircle topoiosmers in the presence of chloroquine.

been identified that contain the alternating purine-pyrimidine sequence motif that is most energetically favored for Z-DNA formation. The SV40 enhancer is an example of an important control region that contains Z-DNA-forming sequences. The transition of these sequences to Z-DNA may play important roles in the function of the enhancer.

Transitions of B-DNA to Z-DNA were investigated here through the use of DNA minicircles. The minicircles were synthesized as relaxed topoisomers, purified, and then supercoiled in incremental steps by treatment with topoisomerase I in the presence of ethidium bromide. The resulting negatively supercoiled topoisomers were resolved by electrophoresis through acrylamide gels in the presence of chloroquine. Topoisomers, which differed by one negative supercoil, were resolved as specific bands. The superhelix density of a given

species was determined by the band counting method (Shure & Vinograd, 1976). The topoisomer preparations were also subjected to gel electrophoresis mobility shift analysis to detect binding of the anti-Z-DNA–Fab. A comparison of the mobilities of the minicircles in the chloroquine gels to the band shift analyses allowed the determination of the superhelix density required to stabilize Z-DNA sequences within specific minicircle topoisomers. The primary advantage in studying the enhancer in minicircles is that the effects of negative supercoiling on specific sequences can be investigated. In a plasmid, or the SV40 genome, sequences that might adopt the Z-DNA conformation compete for the stabilization energy stored as negative supercoils. Therefore, transitions from B-DNA to Z-DNA, which would be difficult to detect in a conventional plasmid, become readily apparent in a DNA minicircle.

To validate our system, two minicircles were synthesized to provide positive (Z^+-minicircle) and negative (Z^--minicircle) controls for the detection of Z-DNA. The resolution of topoisomers for the Z^--minicircles (Figure 1, panel A) revealed the expected bell-shaped distribution. There were no discontinuous transitions from one band to the next. Since the Z^--minicircle has no significant stretches of alternating purine-pyrimidine bases, Z-DNA formation was not expected. However, binding of Fab to the Z^--minicircle was detected at superhelix densities greater than –0.15. However, multiple, mobility-shifted bands were observed consistent with numerous independent B-DNA to Z-DNA transitions. Since Z-DNA was observed only at high levels of superhelix density, all of the independent sequences have a high energy requirement for Z-DNA formation. No single sequence forms Z-DNA more readily than another. Thus, a set of sequences compete for the energy stored as negative supercoils, and many band shifts were observed.

The Z^+-minicircle was identical to the Z^--minicircle with the exception of a $(CG)_{13}$ insert. The Z-DNA insert dramatically affected the topoisomer distribution. In contrast to the continuous bell-shaped distribution observed with Z^--minicircles, a discontinuous distribution was observed, which is the result of the B-DNA to Z-DNA transition of the $(CG)_{13}$ sequence. The transition to the Z-DNA conformation occurred at the –2 topoisomer, which corresponds to a superhelix density of –0.07. This value corresponds with previous results obtained for conventional plasmids by alternate methods such as two-dimensional agarose gel electrophoresis (Ellison et al., 1985, 1986, 1987). Binding of the Fab fragment to the Z^+-minicircle was saturable and resulted in the formation of a unique band shift. This result is consistent with the formation of a monomeric complex between Fab and the unique Z-DNA sequence tract. These experiments demonstrated that the DNA minicircle system has the capacity to detect B-DNA to Z-DNA conversions. In addition, electrophoresis in the presence of chloroquine allowed the resolution of minicircle topoisomers that differ by a single negative supercoil. Therefore, native SV40 sequences can be analyzed by these methodologies to learn more about B-DNA to Z-DNA conversions within the enhancer.

The gel electrophoretic mobility shift analysis of the SV-minicircle clearly demonstrates the presence of Z-DNA at superhelix densities of at least –0.05. A saturation binding experiment was performed with the maximally supercoiled SV-minicircle and Fab to determine the number of Z-DNA sites per minicircle. With increasing Fab concentration, distinct mobility-shifted bands corresponding in molecular weight to monomeric, dimeric, and trimeric complexes of Fab and minicircle DNA were observed. Since only one Fab fragment binds to the $(CG)_{13}$ sequence in the Z^+-minicircle, the observation of trimeric complexes demonstrates that three separate Z-DNA sites are stabilized within the SV40 enhancer. The only sequences with the required alternating purine-pyrimidine motif within the SV-minicircles are the two copies of ATGCATGC and the single copy of ACACACAT.

Confirmation of this assignment comes from the analysis of the SVZ_1-minicircle and the SVZ_2-minicircle. The two minicircles were identical to the Z^--minicircle with the exception of the 24 base pairs of SV40 sequences: The 24 base pair insert consisted of the 8 base pair alternating purine-pyrimidine sequence, flanked on each side with 8 base pairs of the native SV40 sequences. Gel electrophoretic mobility shift analysis demonstrated that each minicircle contained a single Fab binding site. Although the Fab binding patterns were similar, the SVZ_2-minicircle showed Fab binding at superhelix density of –0.10 as compared to the SVZ_1-minicircle, which required a superhelix density of –0.14. Thus, the ACACACAT sequence has a lower energy requirement for the B-DNA to Z-DNA conversion. These results are consistent with the assignment of ATGCATGC and ACACACAT as the Z-DNA-forming sequences within the enhancer-containing minicircle and, by extrapolation, in the native SV40 enhancer.

There was a lack of parity between the negative superhelix density required to generate Z-DNA within the SV-minicircle and the SVZ_1- and SVZ_2-minicircles. The discrepancy may be an indication of the influence of flanking sequences on the B-DNA to Z-DNA transitions. The non-SV40 sequences in the SVZ_1- and SVZ_2-minicircles could be refractory to Z-DNA formation, or may not allow B-DNA to Z-DNA junctions. Conversely, the native SV40 sequences in the SV-minicircle could be Z-DNA-inductive. Therefore, the sequence context of the Z-DNA-forming sites could significantly impact the negative superhelix density required to stabilize Z-DNA.

In the context of an SV40 infection, increases in the negative superhelix density represent the most likely mechanism by which these sequences would be stabilized as Z-DNA. Sufficient levels of DNA unwinding would occur at the initiation of DNA replication. It has been demonstrated that the binding of the large T antigen significantly increases negative superhelix density (Stahl et al., 1986; Dean et al., 1987a; Dodson et al., 1987; Bullock et al., 1989; Roberts, 1989; Gutierrez et al., 1990; Dean & Hurwitz, 1991). In addition, RNA polymerase has been shown to generate high levels of negative superhelix density 5′ to transcriptionally active genes (Wu et al., 1988; Rahmouni & Wells, 1992). Since the SV40 enhancer is located between two transcription units that are in opposite orientations, sufficiently high levels of negative superhelix density could be generated to stabilize short segments of Z-DNA. Wells and co-workers have demonstrated that within *Escherichia coli*, alternating purine-pyrimidine sequences as short as 12 base pairs are stabilized in the Z-DNA conformation when located between two actively transcribed genes on a plasmid (Rahmouni & Wells, 1989). Such a situation exists within the SV40 enhancer, which is located between the early and late transcription units. Moreover, a direct correlation between transcriptional activity and Z-DNA formation has been demonstrated in vitro (Droge & Nordheim, 1991) and in vivo in purified, transcriptionally active, cell nuclei (Wittig et al., 1991).

The SV40 enhancer is essential for both efficient transcription (Benoist & Chambon, 1981; Gruss et al., 1981) and replication (DeLucia et al., 1986; Li et al., 1986; Hertz &

Mertz, 1986); the conversion of B-DNA to Z-DNA within the enhancer could have important regulatory effects. The formation of Z-DNA could have a direct impact by providing binding sites for sequence-specific Z-DNA-interactive proteins. Preliminary data suggest that a Z-DNA binding protein that recognizes the ATGCATGC sequence is copurified with SV40 minichromosomes (Azorin & Rich, 1985). In addition, Z-DNA-interactive proteins, specific for the Z-DNA structural motif regardless of sequence, could interact with Z-DNA within the enhancer. Such Z-DNA-interactive proteins have been detected in a variety of organisms including wheat germ (Lafer et al., 1985b), bull testis (Gut et al., 1987), Drosophila (Nordheim et al., 1982), and tissue culture cells (Leith et al., 1988).

Alternatively, Z-DNA within the enhancer could have an indirect impact: The binding sites for a variety of proteins have been mapped to the enhancer. The nature of the mapping experiments is such that only B-DNA-interactive proteins were included in the analysis (Davidson et al., 1986, 1988; Xiao et al., 1987; Rosales et al., 1987; Fromental et al., 1988). Several binding sites overlap the three Z-DNA sites in the enhancer. Conversion of these sequences to Z-DNA would alter the binding sites for the B-DNA-interactive proteins, preventing them from interacting with their cognate binding sites. Another important indirect effect could result from changes in the helical orientation of protein binding sites as a result of Z-DNA formation. Protein–protein interactions, which occur as a result of DNA looping [for a review, see Matthews (1992)], between proteins bound to distal DNA sequences could be prevented, or promoted, by changes in the spacing of the binding sites with respect to each other. Such changes would be expected if there was a conversion of B-DNA to Z-DNA between two binding sites. In this scenario, a B-DNA to Z-DNA conversion would either disrupt or create an alignment of protein binding sites such that protein–protein interactions could be modulated.

In conclusion, the conversion of B-DNA to Z-DNA within the SV40 enhancer could have important direct and indirect effects on key biological events such as replication and transcription. Both of these processes have dramatic effects on the topology of the DNA. The small stretches of Z-DNA-forming sequences could act as sensors, modulating the activity of other proteins in response to changes in negative superhelix density. However, since the conversion of B-DNA to Z-DNA within the enhancer could have such complex, interdependent effects, the elucidation of the actual interface of these Z-DNA-forming sequences with specific biological activities remains a formidable analytical challenge.

ACKNOWLEDGMENT

We thank all the members of the Rich laboratory for helpful discussions and criticism, especially James McCarthy, Mirriam Sanders, Ky Lowenhaupt, Allan Herbert, and Nassim Usman. Special thanks go to Loren Williams for help with the figures and for his careful review of the manuscript.

REFERENCES

Azorin, F., & Rich, A. (1985) *Cell 41*, 365–374.
Bates, A. D., & Maxwell, A. (1989) *EMBO J. 8*, 1861–1866.
Benoist, C., & Chambon, P. (1981) *Nature 290*, 304–310.
Bullock, P. A., Seo, Y. S., & Hurwitz, J. (1989) *Proc. Natl. Acad. Sci. U.S.A. 86*, 3944–3948.
Davidson, I., Fromental, C., Augereau, P., Wildeman, A., Zenke, M., & Chambon, P. (1986) *Nature 323*, 544–548.
Davidson, I., Xiao, J. H., Rosales, R., Staub, A., & Chambon, P. (1988) *Cell 54*, 931–942.
Dean, F. B., & Hurwitz, J. (1991) *J. Biol. Chem. 266*, 5062–5071.
Dean, F. B., Bullock, P., Murakami, Y., Wobbe, C. R., Weissbach, L., & Hurwitz, J. (1987a) *Proc. Natl. Acad. Sci. U.S.A. 84*, 16–20.
Dean, F. B., Borowiec, J. A., Ishimi, Y., Deb, S., Tegtmeyer, P., & Hurwitz, J. (1987b) *Proc. Natl. Acad. Sci. U.S.A. 84*, 8267–8271.
DeLucia, A. L., Deb, S., Partin, K., & Tegtmeyer, P. (1986) *J. Virol. 57*, 138–144.
DePamphilis, M. L. (1988) *Cell 52*, 635–638.
Dodson, M., Dean, F. B., Bullock, P., Echols, H., & Hurwitz, J. (1987) *Science 238*, 964–967.
Douc-Rasy, S., Kolb, A., & Prunell, A. (1989) *Nucleic Acids Res. 17*, 5173–5189.
Droge, P., & Nordheim, A. (1991) *Nucleic Acids Res. 19*, 2941–2946.
Ellison, M. J., Kelleher, R. J., III, Wang, A. H.-J., Habener, J., & Rich, A. (1985) *Proc. Natl. Acad. Sci. U.S.A. 82*, 8320–8324.
Ellison, M. J., Feigon, J., Kelleher, R. J., III, Wang, A. H.-J., Habener, J., & Rich, A. (1986) *Biochemistry 25*, 3648–3655.
Ellison, M. J., Fenton, M. J., Ho, P. S., & Rich, A. (1987) *EMBO J. 6*, 1513–1522.
Fromental, C., Kanno, M., Nomiyama, H., & Chambon, P. (1988) *Cell 54*, 943–953.
Gruss, P., Dhar, R., & Khoury, G. (1981) *Proc. Natl. Acad. Sci. U.S.A. 78*, 943–947.
Gut, H. S., Bischoff, M., Hobbi, R., & Kuenzle, C. C. (1987) *Nucleic Acids Res. 15*, 9691–9705.
Gutierrez, C., Guo, Z.-S., Roberts, J., & DePamphilis, M. L. (1990) *Mol. Cell. Biol. 10*, 1719–1728.
Hagen, F. K., Zarling, D. A., & Jovin, T. M. (1985) *EMBO J. 4*, 837–844.
Hansen, J. N. (1981) *Anal. Biochem. 116*, 146–151.
Hansen, N. J., Pheiffer, B. H., & Boehnert, J. A. (1980) *Anal. Biochem. 105*, 192–201.
Hertz, G. Z., & Mertz, J. E. (1986) *Mol. Cell. Biol. 6*, 3513–3522.
Keller, W. (1975) *Proc. Natl. Acad. Sci. U.S.A. 72*, 4876–4880.
Lafer, E. M., Sausa, R., & Rich, A. (1985a) *EMBO J. 4*, 3655–3660.
Lafer, E. M., Sausa, R., Rosen, B., Hsu, A., & Rich, A. (1985b) *Biochemistry 24*, 5070–5076.
Leith, I. R., Hay, R. T., & Russell, W. C. (1988) *Nucleic Acids Res. 16*, 8277–8289.
Li, J. J., Peden, K. W., Dixon, R. A. F., & Kelly, T. (1986) *Mol. Cell. Biol. 6*, 1117–1128.
Luchnik, A. N., Bakayev, V. V., Zbarsky, I. B., & Georgiev, G. P. (1982) *EMBO J. 1*, 1353–1359.
Matthews, K. S. (1992) *Microbiol. Rev. 56*, 123–136.
Moller, A., Gabriels, J. E., Lafer, E. M., Nordheim, A., Rich, A., & Stollar, B. D. (1982) *J. Biol. Chem. 257*, 12081–12085.
Moller, A., Nordheim, A., Kozlowski, S. A., Patel, D. J., & Rich, A. (1984) *Biochemistry 23*, 54–62.
Moratta, R., Bremenkamp, M., & Salamini, F. (1983) *Anal. Biochem. 130*, 27–31.
Nordheim, A., & Rich, A. (1983) *Nature 303*, 674–678.
Nordheim, A., & Meese, K. (1988) *Nucleic Acids Res. 16*, 21–37.
Nordheim, A., Tesser, P., Azorin, F., Kwon, Y. H., Moller, A., & Rich, A. (1982) *Proc. Natl. Acad. Sci. U.S.A. 79*, 7729–7733.
Nordheim, A., Pardue, M. L., Weiner, L. M., Lowenhaupt, K., Scholten, P., Moller, A., Rich, A., & Stollar, B. D. (1986) *J. Biol. Chem. 261*, 468–476.
Nordheim, A., Herrera, R. E., & Rich, A. (1987) *Nucleic Acids Res. 15*, 1661–1677.
Peck, L. J., Nordheim, A., Rich, A., & Wang, J. C. (1982) *Proc. Natl. Acad. Sci. U.S.A. 79*, 4560–4564.

Peck, L. J., Wang, J. C., Nordheim, A., & Rich, A. (1986) *J. Mol. Biol. 190*, 125–127.
Rahmouni, A. R., & Wells, R. D. (1989) *Science 246*, 358–363.
Rahmouni, A. R., & Wells, R. D. (1992) *J. Mol. Biol. 223*, 131–144.
Roberts, J. M. (1989) *Proc. Natl. Acad. Sci. U.S.A. 86*, 3939–3943.
Rosales, R., Vigneron, M., Macchi, M., Davidson, I., Xiao, J. H., & Chambon, P. (1987) *EMBO J. 6*, 3015–3025.
Runkel, L., & Nordheim, A. (1986) *J. Mol. Biol. 189*, 487–501.
Scholer, H. R., & Gruss, P. (1984) *Cell 36*, 403–411.
Singleton, C. K., Klysik, J., Stirdivant, S. M., & Wells, R. D. (1982) *Nature 299*, 312–316.
Stahl, H., Droge, P., & Knippers, R. (1986) *EMBO J. 5*, 1939–1944.
Wittig, B., Dorbic, T., & Rich, A. (1991) *Proc. Natl. Acad. Sci. U.S.A. 88*, 2259–2263.
Wu, H., Shyy, S., Wang, J. C., & Liu, L. F. (1988) *Cell 53*, 433–440.
Xiao, J. H., Davidson, I., Ferrandon, D., Rosales, R., Vigneron, M., Macchi, M., Ruffenach, F., & Chambon, P. (1987) *EMBO J. 6*, 3005–3013.
Zarling, D. A., Arndt-Jovin, D. J., Robert-Nicoud, M., McIntosh, L. P., Thomae, R., & Jovin, T. M. (1984) *J. Mol. Biol. 176*, 369–415.